



ORIGINAL ARTICLE

Perspectives on composite films of chitosan-based natural products (Ginger, Curcumin, and Cinnamon) as biomaterials for wound dressing



Khadiga Ahmed Ismail ^a, Ahmad El Askary ^a, M.O. Farea ^b, Nasser S. Awwad ^c, Hala A. Ibrahim ^{d,e}, Moustapha Eid Moustapha ^f, A.A. Menazea ^{g,*}

^a Department of Clinical Laboratory Sciences, College of Applied Medical Sciences, Taif University, P.O. Box 11099, Taif 21944, Saudi Arabia

^b Department of Physics, Faculty of Science, IBB University, Yemen

^c Chemistry Department, Faculty of Science, King Khalid University, P.O. Box 9004, Abha 61413, Saudi Arabia

^d Biology Department, Faculty of Science, King Khalid University, P.O. Box 9004, Abha 61413, Saudi Arabia

^e Department of Semi Pilot Plant, Nuclear Materials Authority, P.O. Box 530, El Maadi, Egypt

^f Department of Chemistry, College of Science and Humanities, Prince Sattam bin Abdulaziz University, Alkharj, Saudi Arabia

^g Spectroscopy Department, Physics Research Institute, National Research Centre, Dokki, 12622 Giza, Egypt

Received 13 December 2021; accepted 17 January 2022

Available online 20 January 2022

KEYWORDS

Chitosan;
Ginger;
Curcumin;
Cinnamon;
Antimicrobial Activity

Abstract Natural materials are gaining popularity in wound healing and food applications, and they have the potential to alleviate the major environmental problems generated via traditional materials. Biomaterials based on Chitosan incorporated with natural products (Ginger, Curcumin, and Cinnamon) have been fabricated by solvent casting method. The antimicrobial characterization of the prepared samples were also investigated using in vitro antimicrobial studies using Gram-positive microorganism [*Micrococcus luteus*, *Staphylococcus aureus*, and *Staphylococcus epidermidis*], Gram-negative microorganism [*Pseudomonas aeruginosa*], and pathogenic [*Candida albicans*]. XRD patterns confirmed the complexation between chitosan and other natural products and this indicate the change in structural of chitosan. The shifting and disappearing of bands in FTIR-ATR and changing in fingerprints in FTIR spectra indicate the homogeneity and interaction between chitosan and the other. Optical properties such as absorption, absorption coefficient, Urbach tail and band gap calculation confirmed that Ginger, Curcumin and Cinnamon interact with chitosan and induces localized state between valence and conduction band. The mechanical properties also studied and revealed that Chitosan/Ginger has the best mechanical characteristic

* Corresponding author

E-mail address: aanter7@gmail.com (A.A. Menazea).

Peer review under responsibility of King Saud University.



compared the other samples. In addition, the shifting toward higher wavelength for chitosan/Ginger may be utilized to generate electron-hole pairs, which is important for antimicrobial activities, and this confirmed from antimicrobial analysis that Chitosan/Ginger give high antimicrobial activity toward Gram-positive microorganism and suggest it for wound dressing application.

© 2022 Published by Elsevier B.V. on behalf of King Saud University. This is an open access article under the CC BY-NC-ND license (<http://creativecommons.org/licenses/by-nc-nd/4.0/>).

1. Introduction

The world now searches for creating new biomaterials based on safe natural products with high antimicrobial activities to prevent the spread of bacteria and viruses. Those materials can regulate hazardous bacterial growth. They contain an antimicrobial agent, which inhibits microorganisms' stability to grow in the material (Liu et al., 2021).

Chitosan and its derivatives are attracting the attention of researchers for many decades because of its antimicrobial activity that helps scientists to develop it to improve its antimicrobial properties (Lin et al., 2019; Zou et al., 2019). Chitosan is a non-toxic polymer that can be modified to increase its antimicrobial properties by blending or doping with metal oxides to enhance their physicochemical properties that make it has polycation nature (M, y., & pr, i., 2019). Because of its antibacterial properties, chitosan is a good contender for usage as a packaging material. Other natural materials can be used to improve the film-forming characteristics, which will add to the antibacterial qualities (Ah et al., 2014). Chitosan has piqued the interest of researchers not only because of its large variety antibacterial activity, but also because it is the most biocompatible, and biodegradable polymeric substance with a tremendous material complexation capabilities.

The antibacterial biopolymer films based on chitosan and various natural products (Ginger, Curcumin, and Cinnamon), which were proved to inhibit the growth of bacteria in an *in vitro* study. The use of antibiotics against bacteria is an important form of treatment of different types of bacteria but often causes adverse problems. Earlier studies have investigated that ginger play a crucial role in microbial growth prevention, or serve as antimicrobial agents (Yang et al., 2021).

Significant research on ginger has shown that ginger has antimicrobial activity (Ah et al., 2014). Curcumin is a natural compound known as turmeric and widely used for medicinal purposes. It was used for decades to treat many inflammatory and other diseases, and its non-toxicity has gained considerable interest, even at high doses (Mottterlini et al., 2000). Cinnamon shows antimicrobial activity that was assigned to the characteristic of bioactive phytochemicals including cinnamaldehyde and eugenol. When used incorrect conditions, cinnamon is not harmful. In addition, it may be utilized in the treatment of bacterial antibiotic-resistant infections (Nabavi et al., 2015).

A. Irawan et al. (Irawan et al., 2019) investigated the influences of chitosan/red ginger as just an active plastic packaging for food safety. A. Amalraj et al. (Amalraj et al., 2020) investigated the antibacterial efficacy of chitosan/gum arabic/polyethylene glycol composite doped by black pepper and ginger essential oils for wound dressing and packaging. M. Yashaswini et al. (Yashaswini and Iyer,

2019) obtained the influences of doping of turmeric/clove/ginger on Chitosan for food applications. P. Rachtanapun et al. (Rachtanapun et al., 2021) discussed the influences of doping of Curcumin extract by chitosan film and found that it has high activity for packaging. S. Chakraborty et al. (Chakraborty and Ilagan, 2020) prepared film consistent of chitosan and curcumin to use it as a sensor to detect fluoride and o-nitrophenol and N. V. Cuong et al. (Rachtanapun et al., 2021) performed the influence of Curcumin on Chitosan-PAA Silver to be used as wound dressing, antimicrobial packaging and antibacterial materials.

Wound infections can hinder the process of healing, and if not treated, they can progress to infection. The human tissue serves as a protection towards different forces, but when it is damaged, it loses its effectiveness and gets susceptible to bacterial microorganisms (Matica et al., 2019). The perfect treatment is clean, non-toxic, and antimicrobial, as well as reflecting a physical barrier that is selectively permeable while maintaining or providing a suitable atmosphere; providing a suitable tissue temperature to favour epithelial movement and tissue formation; and non-adherent to avoid traumatic separation upon recovery (Dhivya et al., 2015). The best antibacterial polymeric must be easy to create and inexpensive, stable for long-term usage, non-toxic and biodegradable, and, greatest significantly, biocidal against a variety of diseases. (Kenawy et al., 2007). Furthermore, chitosan-based products differ from typical dressings such as gauze or cotton wool in that chitosan actively assists in the healing of wounds (Ji et al., 2020). Chitosan derivatives have been useful in a variety of fields, including water purification, most significantly, medicine and pharmacy (Zhang et al., 2022). Allan et al. (Allan and Hadwiger, 1979) were among the first to suggest that chitosan has antibacterial properties, and the idea of producing chitosan derivatives has grown in popularity among academics since then.

Herein, in our study, we will synthesis a biomaterials based on chitosan and natural products such as: Ginger, Curcumin, and Cinnamon. The antibacterial activity of the synthesized biomaterials has been performed to examine the impact of these products to decide and gauge which of them is the best impact in improving the antibacterial activity of chitosan for has utilized in the food backing and wound dressing as low-cost natural materials.

2. Experimental Work:

2.1. Materials:

Chitosan (M. W. = 160 kDa) 82% degree of deacetylation (DD) was purchased from ALAMIA company for chemicals. Ginger, Curcumin, and cinnamon were bought from Sigma-Aldrich in powder form.

2.2. Fabrication of Chitosan blended with Ginger, Curcumin and Cinnamon:

Firstly, all powders used are dried at 50 °C to remove any moisture. Chitosan was dissolved in Double Distilled Water containing 2% acetic acid, then stirred continuously at 50 °C until homogeneous transparent viscous liquid was obtained. Equal amounts (0.5 gm) of (Ginger, Curcumin, and Cinnamon) in powder form are added to the Chitosan solution under vigorous stirring at 50 °C for 6 hrs and sonicated for 10 min using a water bath type sonicator to confirm the miscibility between Chitosan and other components. Then the prepared solutions are cast in Petri dishes and placed in an oven at 40 °C for about Two days for drying. The obtained films have been kept in vacuum desiccators until use. The thickness of the prepared films was in the range 0.1 mm to 0.2 mm.

2.3. Characterization techniques:

X-ray diffraction was performed via X-ray diffractometer (analytical-x' pertpro, Cu $k_{\alpha 1}$ radiation, $\lambda = 1.5404 \text{ \AA}$, 45 kV) within $\theta = 5\text{--}80^\circ$. FTIR-ATR spectral data are collected via Vertex 80 Bruker (made in Germany) at room temperature in the range $4000\text{--}400 \text{ cm}^{-1}$. UV/vis. Spectral data were collected using Jasco 570 double-beam spectrometer within the range of 200–1000 nm. Morphological analysis of samples has been examined by FESEM type (Quanta FEG 250, USA). The tensile strength test was performed using an LLOYD LR 10 k universal testing machine in England, according to TAPPI (T494-06) standard procedure.

2.4. The antimicrobial activity

Bacteria used in this study were Gram-positive microorganism [*Micrococcus luteus* (ATCC 10240), *S. aureus* (ATCC 6538), and *S. epidermidis* (ATCC 12228)], Gram-negative microorganism [*Pseudomonas aeruginosa* (ATCC 27853)] and pathogenic fungi [*Candida albicans* (ATCC 12228)]. All microorganisms are freshly overnight broth cultures that have been incubated at 37 °C. Each plate contained 20.0 mL of sterile nutrient agar medium that was infected with microorganism suspensions (Mostafa et al., 2016; McFarland, 1907)(Gao et al., 2019). After that the media had cooled and solidified, the prepared films had been divided into two groups: one was attached to the surface of the previously synthesized inoculated agar plates, while the second group was used in the shake flask method applying 25.0 μL of microorganisms suspensions have been inoculated into each plate containing 20.0 mL of the sterile nutritional agar medium (NA), and the inoculum size of both pathogenic strains was adjusted to roughly 0.5 McFarland standard (1.5 10⁸ CFU /mL). The seeded plates had been chilled for one hour before being incubated at 37 °C for 24 h, and the zone of inhibition was observed (ZI) have been measured in millimeters. The antimicrobial activity was measured throughout the relative [%] reduction of the growth of these selected pathogenic strains was detected by optical density (OD) at 600.0 nm and the antimicrobial activity was measured throughout the relative [OD (%)] reduction of these pathogenic strains after treated with the disc samples compared to the control of these pathogenic strains have no any treatment(Yan et al., 2020; Yang

et al., 2017). The following equation was used to express all of the results (Rehim et al., 2020; Abdelghaffar et al., 2018) and tabulated in the following Tables 3 and 4.

$$\text{Relative[ODReduction(\%)]} = (A - B/A) \times 100 \quad (4)$$

Where A is the (OD) of the control flask contains pathogenic strains only without any treatment and B is the (OD) of tested flasks after applying a disc sample treated.

3. Results and discussion:

3.1. X-ray diffraction (XRD)

Fig. 1 represents XRD of Chitosan, Chitosan/Ginger, Chitosan/Curcumin and Chitosan/Cinnamon. For Chitosan, there are diffraction peaks at $2\theta = 7.2^\circ$ and 20.5° (Mohseni-Bandpi et al., 2015; Choo et al., 2016; Olafadehan et al., 2019). When Ginger, Curcumin and Cinnamon added

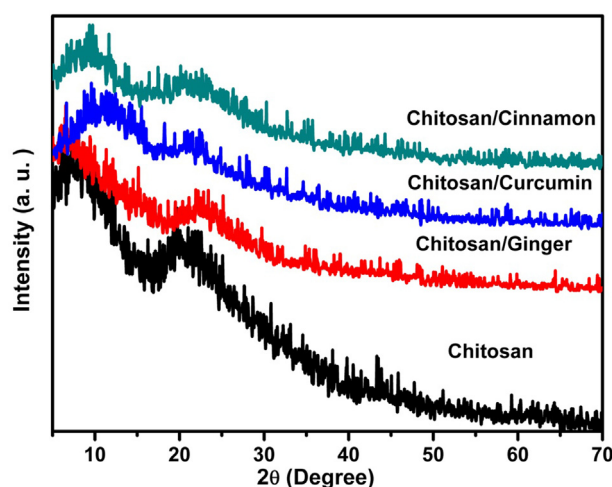


Fig. 1 XRD diffraction patterns of Chitosan, Chitosan/Ginger, Chitosan/Crucumin and Chitosan/Cinnamon.

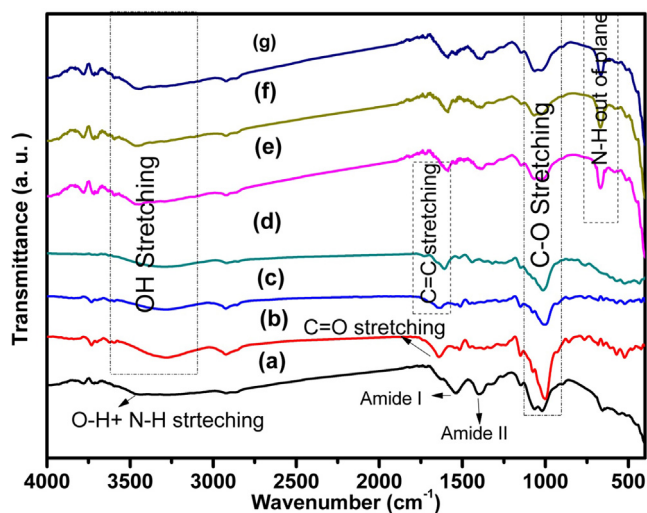


Fig. 2 FTIR-ATR of (a) Pure Chitosan, (b) Ginger, (c) Curcumin, (d) Cinnamon, (e) Chitosan/Ginger, (f) Chitosan/Curcumin, and (g) Chitosan/Cinnamon.

to the chitosan, the diffraction peaks appeared flatter and less visible, indicating a loss in crystallinity with addition of Ginger, Curcumin and Cinnamon. In addition, there is a noticeable shift to a higher 2θ in addition when these compounds are added to chitosan, the crystallinity index decreases, resulting in less close packing in the polymer chains. This could be due to a stronger interaction between active chemicals and biopolymers (i.e. H-bonds, Van der Waals), which improves the crystalline 3D-network.

3.2. Fourier transform infrared –Attenuated total reflection analysis (FTIR-ATR):

Fig. 2 shows FTIR-ATR of Chitosan, Ginger, Curcumin, Cinnamon, Chitosan/Ginger, Chitosan/Curcumin and Chitosan/Cinnamon. FTIR-ATR of Chitosan obtains a band at 3454 cm^{-1} , which is assigned to O-H and N-H stretching vibrations. Bands at 2920 cm^{-1} and 2865 cm^{-1} are corre-

sponded to CH symmetric and asymmetric stretching vibration, respectively. The bands at 1631 cm^{-1} and 1542 cm^{-1} are due to amide I (C = O) and amide II (N-H bending vibration), respectively. The band at 1402 cm^{-1} corresponds to the –OH group of the primary alcoholic group. The stretching of the C-O-N group is observed at 1324 cm^{-1} . The band at 1147 cm^{-1} is attributed to the asymmetric stretching of bridge oxygen (glycosidic bonds). Bands at 1067 cm^{-1} and 1020 cm^{-1} corresponded to C-O in the secondary and primary O-H groups, respectively. The band at 655 cm^{-1} is attributed to N-H out of the plane (Wang et al., 2018, 2021). Ginger obtains a band at 3282 cm^{-1} corresponds to the O-H stretching vibration. Asymmetric stretching of CH_2 is observed at 2923 cm^{-1} . The band at 1640 cm^{-1} has related to O-H bending vibration and stretching vibration of the C-O bond. The stretching vibration of C = C of an aromatic ring is seen at 1516 cm^{-1} . Bands at 1149 cm^{-1} , 1082 cm^{-1} , and 1000 cm^{-1} are assigned to C-O-C stretching vibration (Feng et al., 2021; Li

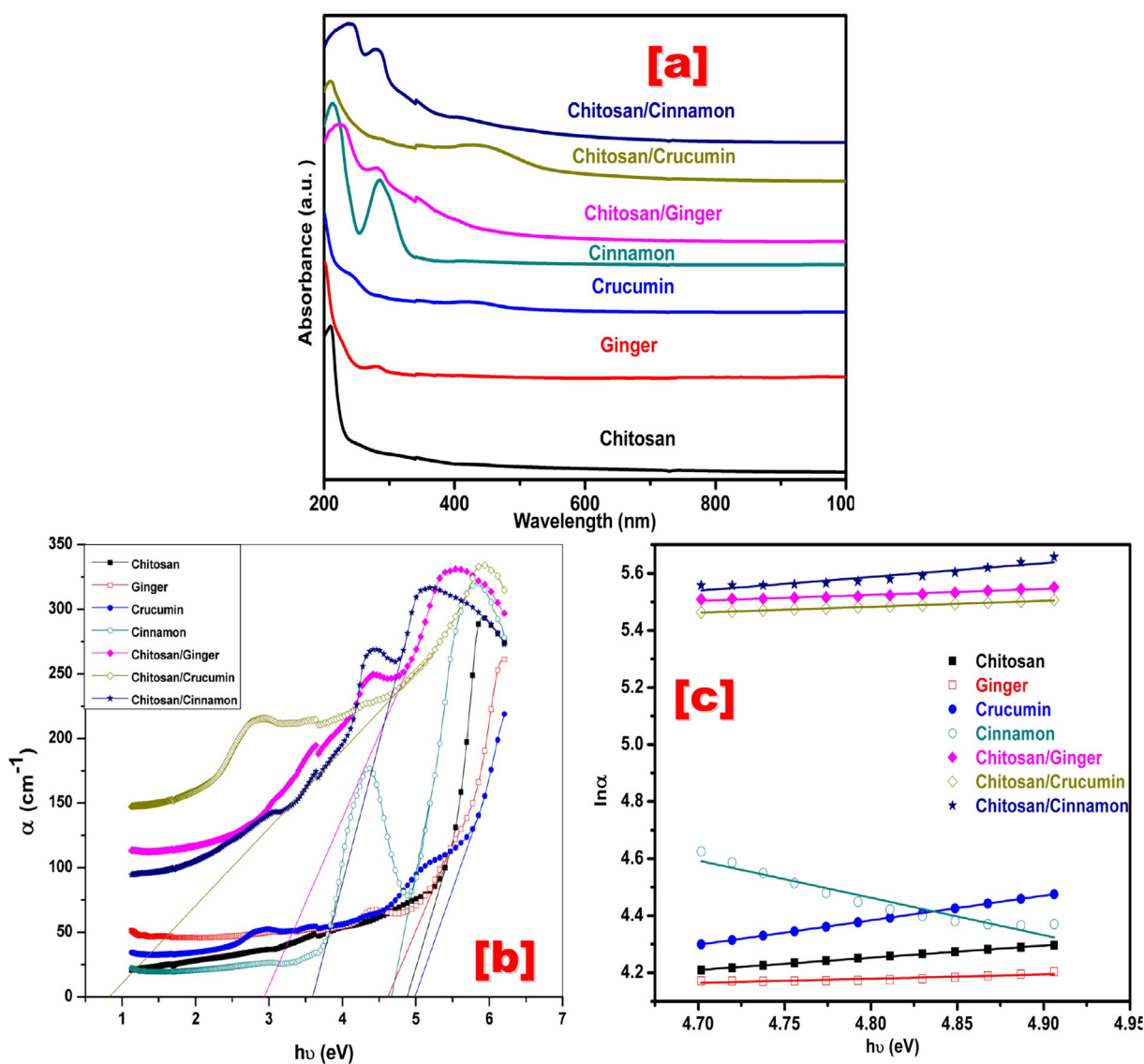


Fig. 3 (a) UV-Vis absorption spectra, (b) Relation between α and $h\nu$, and (c) Relation between $\ln \alpha$ and $h\nu$ of Chitosan, Ginger, Curcumin, Cinnamon, Chitosan/Ginger, Chitosan/Curcumin and Chitosan/Cinnamon.

and Wang, 2021; Zhang et al., 2021). Curcumin shows a band at 3284 cm^{-1} , which corresponds to O-H stretching. Bands at 2924 cm^{-1} and 2850 cm^{-1} have corresponded to CH_2 symmetric and asymmetric stretching vibration. The band at 1631 cm^{-1} corresponds to the overlapping of stretching vibrations of $\text{C}=\text{C}$ and $\text{C}=\text{O}$. While the band at 1512 cm^{-1} indicates the existence of ethylene group in Curcumin. The band at 1277 cm^{-1} is related to C-O (phenolic band) bending vibration (Ji et al., 2021). C-O-C stretching vibrations are seen at 1149 cm^{-1} , 1074 cm^{-1} , and 1000 cm^{-1} (Duan et al., 2021). C-H band is observed at 856 cm^{-1} and 761 cm^{-1} (Ismail et al., 2014; Valand et al., 2015; Chen et al., 2015; Yaseen et al., 2020). Cinnamon shows a stretching vibration band at 3296 cm^{-1} corresponding to O-H of alcohols and phenols. The C-H stretching vibration of alkanes is observed at 2919 cm^{-1} . The weak band at 1736 cm^{-1} corresponds to the stretching vibration of $\text{C}=\text{O}$ of aldehydes. The presence of $\text{C}=\text{C}$ (alkenes) is shown at 1608 cm^{-1} . The absorption band at 1440 cm^{-1} is attributed to the bending vibration of C-OH of alkanes.

The band at 1014 cm^{-1} has corresponded to C-O stretching vibration. The $\text{C}\equiv\text{C}$ -H bending vibration was saw at 767 cm^{-1} (Salim and Bidin, 2017; Zhang et al., 2016). The change in intensity, shifting of bands, appearing and/or disappearing of bands in FTIR indicating the complexation and miscibility between components of materials so that FTIR is a very useful technique for indicating the bond breaking and this confirmed the interaction between materials.

As seen in Chitosan/Ginger, Chitosan/Curcumin and Chitosan/Cinnamon spectrum that O-H stretching band at 3447 cm^{-1} , which shifted to higher wavenumber, compared to that for individual materials. The bands at 1631 cm^{-1} and at 1516 cm^{-1} vanished and a new band appeared at 1585 cm^{-1} . The intensity of the band at 667 cm^{-1} is increased compared to chitosan.

3.3. Optical properties

Fig. 3a shows UV-Vis spectra of Chitosan, Ginger, Curcumin, Cinnamon, Chitosan/Ginger, Chitosan/Curcumin and Chitosan/Cinnamon at room temperature in the range 200–1000 nm. As seen in Fig. 3a, Chitosan has a maximum band at 208 nm, which corresponds to N-acetyl glucosamine and glucosamine of Chitosan (Liu et al., 2006; Guo et al., 2013). Ginger shows a band at 280 nm, which indicates the presence of both flavone and gingers in ginger (Singh et al., 2014). Curcumin shows two bands at 245 nm and 422 nm because of the π - π^* type excitation resulting from the electronic dipole. As there are electrostatic interactions between polar

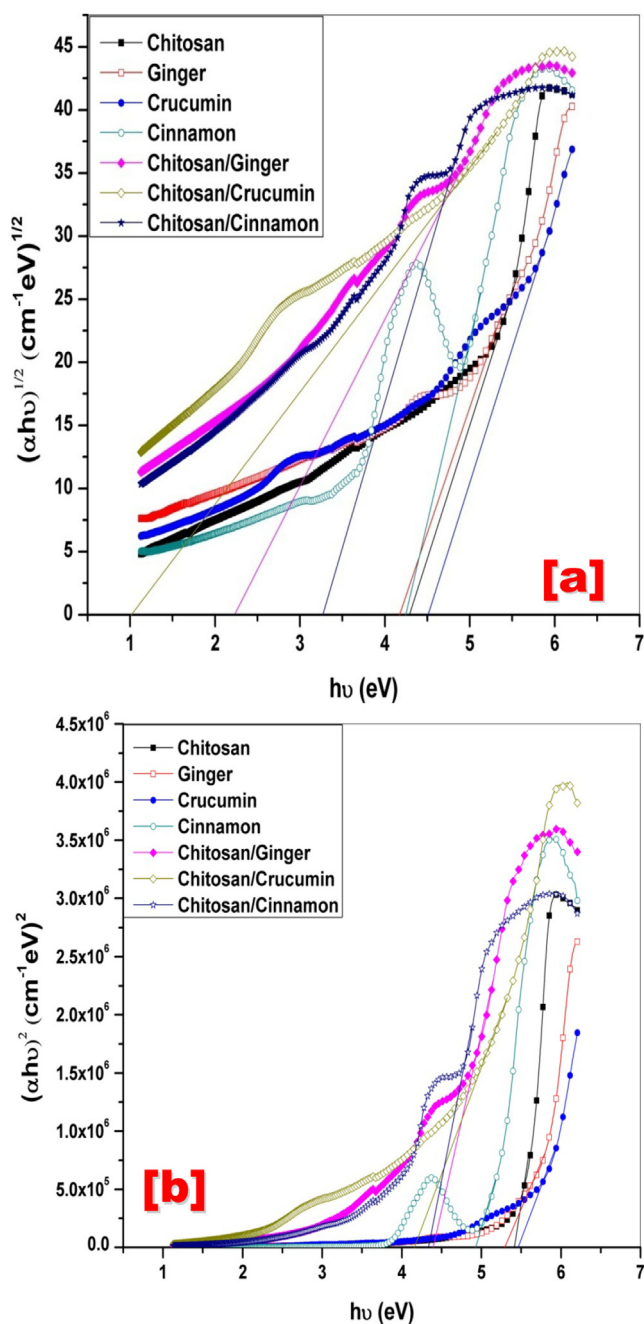


Fig. 4 Relation between (a) $(\alpha h\nu)^{1/2}$ and (b) $(\alpha h\nu)^2$ versus $h\nu$ of Chitosan, Ginger, Curcumin, Cinnamon, Chitosan/Ginger, Chitosan/Curcumin and Chitosan/Cinnamon.

Table 1 Values of absorption edge, band tail energy, direct (E_{gi}), indirect (E_{gd}) optical band gap energy.

Samples	Absorption edge (eV)	Band Tail (eV)	Energy Gap (eV)	
			E_{gd}	E_{gi}
Chitosan	4.88	1.53	5.41	4.28
Ginger	4.61	0.94	5.29	4.15
Curcumin	4.98	2.97	5.45	4.49
Cinnamon	4.65	0.44	4.93	4.24
Chitosan/Ginger	2.91	6.53	4.39	2.25
Chitosan/Curcumin	0.80	5.13	4.15	1.00
Chitosan/Cinnamon	3.58	3.24	4.31	3.26

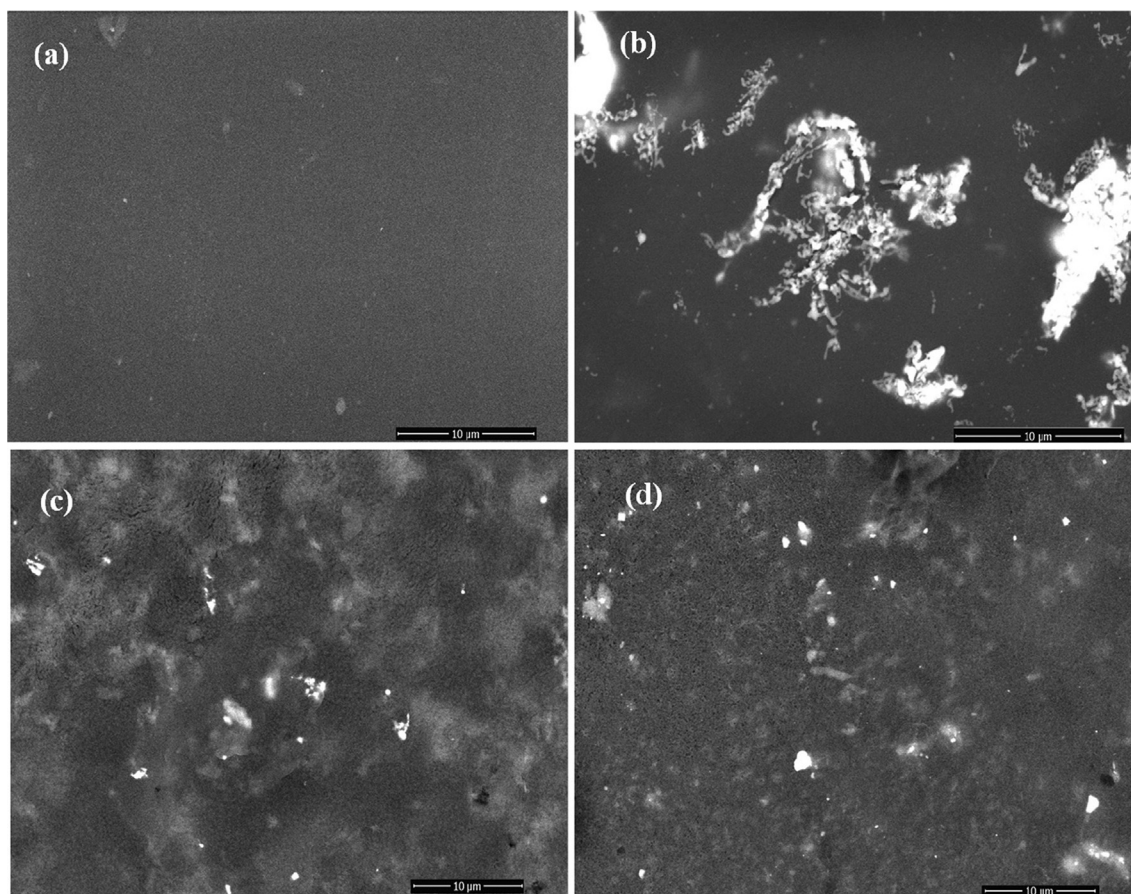


Fig. 5 FE-SEM photos of Chitosan, Chitosan/Ginger, Chitosan/Curcumin and Chitosan/Cinnamon.

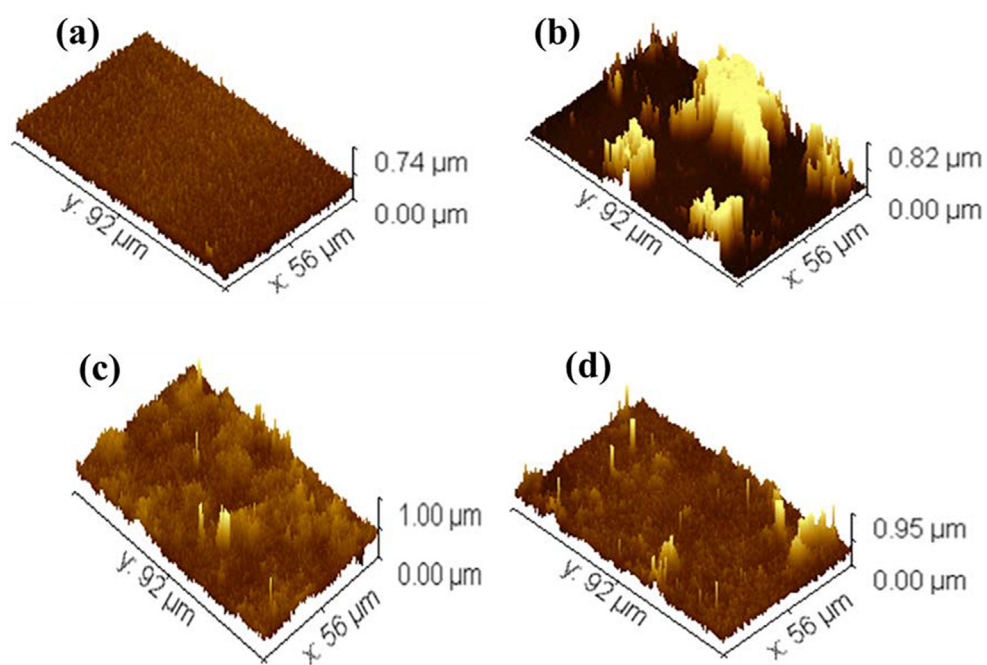


Fig. 6 3D images of (a) Chitosan, (b) Chitosan/Ginger, (c) Chitosan/Curcumin and (d) Chitosan/Cinnamon.

chromophores in Curcumin and molecules and solvent due to the degradation of Curcumin in water (Subhan et al., 2014; Bonilla and Sobral, 2017). Cinnamon shows also two absorption bands at 213 nm and 284 nm due to π - π^* of the conjugated C = C and C = O bonds (Aziz, 2017). For Chitosan/Ginger, there is a shift in the band of chitosan to a longer wavelength (red shift) from 208 nm to 223 nm. While for Chitosan/Curcumin and Chitosan/Cinnamon, new bands are appearing at 439 nm and 409 nm, respectively. This means the presence of surface plasmon resonance phenomena for Chitosan blended with both Curcumin and Cinnamon. These results indicate the interaction and complexation between chromophoric functional groups of Ginger, Curcumin, and Cinnamon with chitosan and this agreed with FTIR-ATR results.

Major information about the band gap and the band structure between different materials can be estimated from the calculation of optical absorption parameters such as optical absorption coefficients (α) and it is calculated from the following equation (Menazea et al., 2020).

$$\alpha(\lambda) = \frac{2.303}{t} A \quad (1)$$

Where A is the absorbance and t is the thickness of the prepared sample. Fig. 3b obtains the relation between α and $h\nu$ (photon energy) for Chitosan, Ginger, Curcumin, Cinnamon, Chitosan/Ginger, Chitosan/Curcumin, and Chitosan/Cinnamon. The extrapolation of the linear portion of the curve with $h\nu$ (x-axis) gives absorption edge values and it is tabulated in Table 1. As seen from the table that the value of absorption edge shifted to lower photon energy compared to individual components and this means a reduction in bandgap structure of Chitosan and other components and also due to charge transfer complexes between different Chitosan and other materials.

Amorphous materials are characterized by their band tail energy E_y and have the property that their electronic transition density decreases exponentially with the band tail energy between located states. Therefore, it can calculate the band tail energy by calculating the reciprocal of the slope that results from drawing between $\ln \alpha$ and $h\nu$ as showed in Fig. 3c according to Urbach relation (Mott and N. F. Davis NF, , 1979).

$$\alpha = \alpha_0 \exp\left(\frac{h\nu}{E_y}\right) \quad (2)$$

As shown in Table 1 that Urbach energy values are increased with chitosan blends compared with other individual components and this means that there is a structural disorder resulting from intermolecular interaction and random fluctuation of internal fields between chitosan and other components.

The bandgap energy values that result from optical transition might be estimated by Mott and Davis extrapolation method that occurred [46]:

Table 2 Values of root mean square roughness (Rq) and mean roughness (Ra) for Chitosan, (b) Chitosan/Ginger, (c) Chitosan/Curcumin and (d) Chitosan/Cinnamon.

Samples	Root mean square roughness (Rq)	Mean roughness (Ra)
Chitosan	50.6 nm	40.1 nm
Chitosan/Ginger	224.7 nm	167.2 nm
Chitosan/Curcumin	82.3 nm	63.1 nm
Chitosan/Cinnamon	80.0 nm	53.5 nm

Table 3 Antimicrobial activity of Chitosan, Chitosan/Ginger, Chitosan/Curcumin and Chitosan/Cinnamon via agar plate method.

Test bacteria	Samples			
	Inhibition zone (mm)			
	Chitosan	Chitosan/Ginger	Chitosan/Curcumin	Chitosan/Cinnamon
<i>Pseudomonas aeruginosa</i>	NiL	NiL	NiL	NiL
<i>Micrococcus luteus</i>	NiL	NiL	NiL	NiL
<i>S. aureus</i>	NiL	NiL	NiL	NiL
<i>S. epidermidis</i>	NiL	16.0	15.0	Nil
<i>Candida albicans</i>	NiL	NiL	NiL	NiL

* Nil: No antimicrobial activity recorded.

Table 4 Antimicrobial activity of Chitosan, Chitosan/Ginger, Chitosan/Curcumin and Chitosan/Cinnamon via shake flask method.

Test bacteria	Samples			
	Treated sample			
	Chitosan %	Chitosan/Ginger %	Chitosan/Curcumin %	Chitosan/Cinnamon %
<i>Pseudomonas aeruginosa</i>	NiL	58.97	NiL	NiL
<i>Micrococcus luteus</i>	62.50	95.51	93.59	33.01
<i>S. aureus</i>	23.74	9.29	NiL	11.87
<i>S. epidermidis</i>	NiL	96.26	84.62	NiL
<i>Candida albicans</i>	44.98	17.27	46.94	41.64

* Nil: No antimicrobial activity recorded.

$$(\alpha hv) = B(hv - E_g)^{1/n} \quad (3)$$

Where B is regarded to the probability of transition (assumed to be constant) and n is regarded to the distribution of state density, thus defining the form of electronic transition. The plot of both direct and indirect transition against hv is seen in Fig. 4. As seen from values in Table 1 that there are clear decreases in values of direct and indirect optical band gap energy of chitosan blends compared to individual materials. This results meaning that there is electronic interaction between Chitosan and other component resulting to increase the number of localized charge carrier levels (trapping sites) leading to a decrease in the structural order of the system and this confirmed the complexation and interaction between a different components of the system.

3.4. Morphological

Fig. 5 (a-d) shows FE-SEM images of the morphology of pure Chitosan and Chitosan doped by Ginger, Curcumin, and Cinnamon samples, respectively. Fig. 5a obtains the homogenous coherent nature of chitosan. Fig. 5b shows the original fiber of raw ginger granules scattered in chitosan with slight agglomeration. The agglomeration of Ginger could be evident from polymer adherence and magnetic interaction between the particles. Fig. 5c and 5d shows a uniform distribution of both Curcumin, and Cinnamon on chitosan surface with appearing

of small white spot on some parts of the image because of small agglomeration that related to the percentage of addition of Curcumin, and Cinnamon.

The surface roughness of the produced membranes was studied using 3D image using Gwyddion software are seen in Fig. 6. The brightest area in these photos depicts the membrane's highest point, while the dark areas depict the valleys or membrane pores. Table 2 summarizes the surface roughness characteristics. As seen R_q and R_a is increased compared to pure chitosan which means that surface properties are enhanced. As noticeable Chitosan/Ginger has higher roughness compared to other samples which depicts that has high antibacterial activity.

3.5. Antimicrobial activity of films:

As seen from Figs. 7, 8, and Table 3 the agar plate method is not effective for measuring antimicrobial activity for prepared films so the shake flask method is used. In this experiment, the samples Chitosan/Ginger and Chitosan/Curcumin have excellent antimicrobial activity on gram-positive microorganism and moderate antimicrobial activity toward *Candida albicans* respectively, while the sample Chitosan and Chitosan/Cinnamon have moderate antimicrobial activity toward the pathogenic microorganism strains and very good antimicrobial activity toward *Candida albicans*. Activity index of Chitosan, Chitosan/Ginger, Chitosan/Curcumin and Chitosan/Cinna-

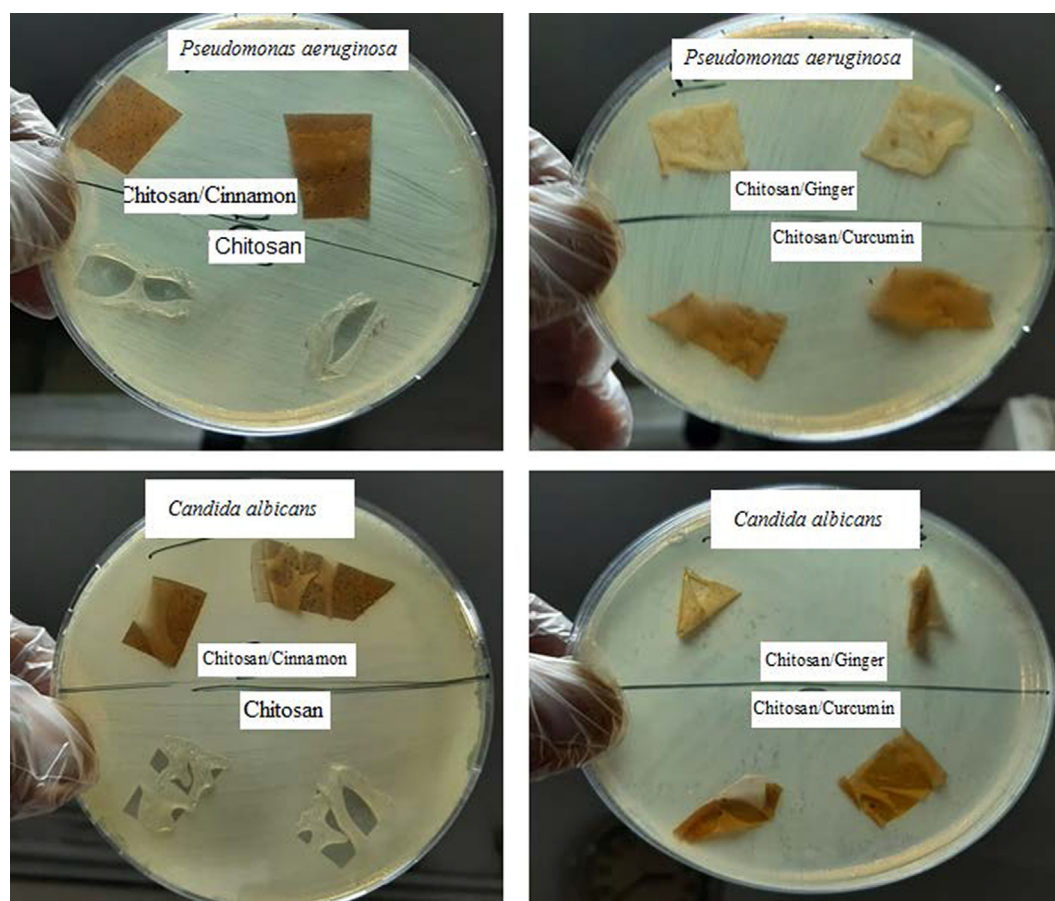


Fig. 7 Antimicrobial activity of Chitosan, Chitosan/Ginger, Chitosan/Curcumin and Chitosan/Cinnamon against *Pseudomonas aeruginosa* and *Candida albicans* via agar plate method.

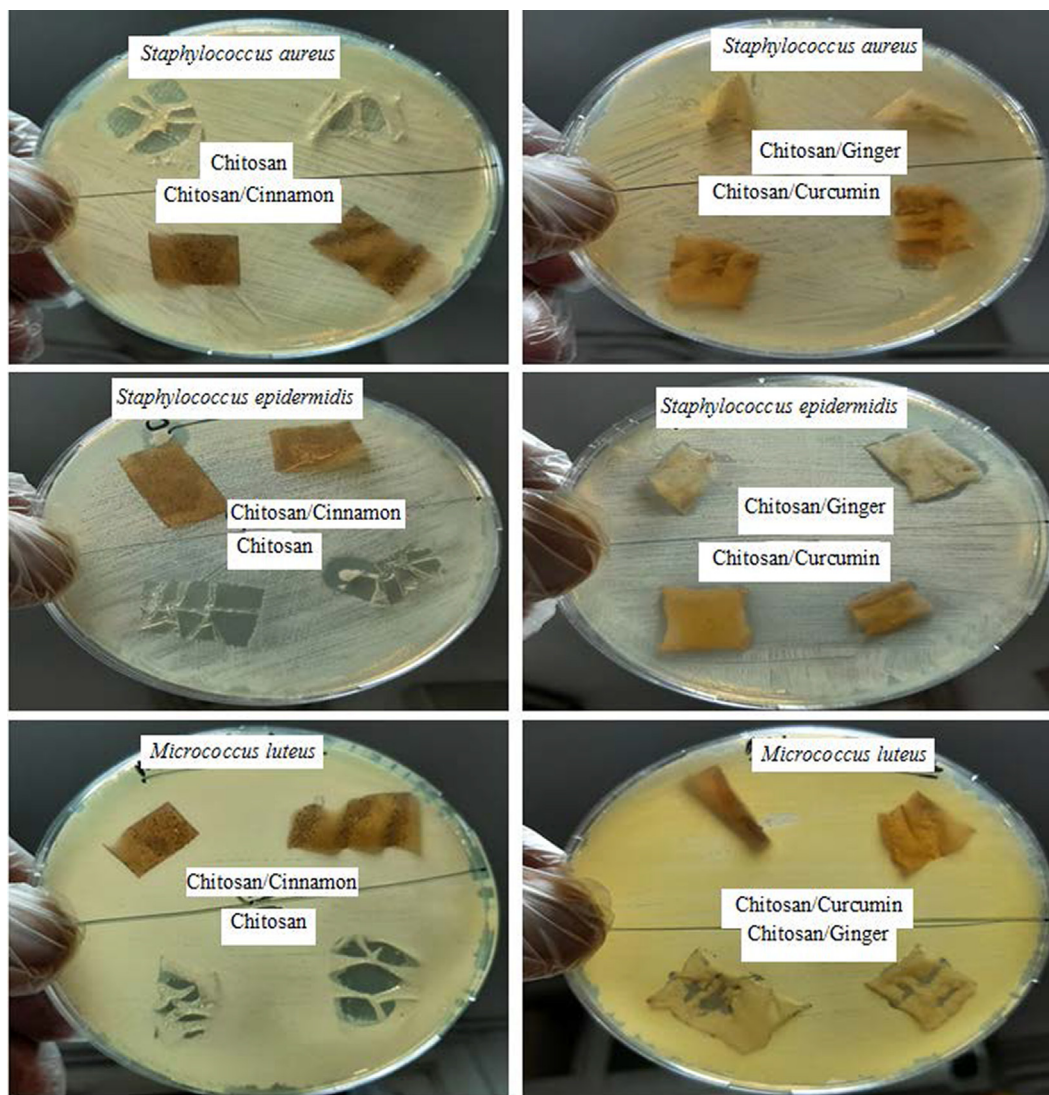


Fig. 8 Antimicrobial activity of Chitosan, Chitosan/Ginger, Chitosan/Curcumin and Chitosan/Cinnamon against *Staphylococcus aureus*, *Staphylococcus epidermidis* and *Micrococcus luteus* via agar plate method.

mon against *Staphylococcus aureus*, *Staphylococcus epidermidis* and *Micrococcus luteus* was obtained in Fig. 9 as statistical data.

The manner of action of these samples may cause suppression of the microorganism cell wall, which is composed of peptidoglycan, a muco polysaccharide component (murein). So, the influence of these substances on gram-positive microorganism cell walls, that entered the microorganism cell and halted several cascading actions including inhibition of nucleic acid synthesis, that led to protein formulation inhibition, and then inhibition of other microorganism metabolism activities. These specimen are also antibacterial against pathogenic (*Candida albicans*), Chitosan /Ginger, has an excellent antimicrobial activity toward both gram-positive microorganism (*Micrococcus luteus*, *S. aureus*, and *S. epidermidis*), gram-negative microorganism (*Pseudomonas aeruginosa*) and pathogenic *Candida albicans* with reduction (%) rang (17.27 – 96.26) for Chitosan/Ginger, the other samples (Chitosan/Curcumin) that has reduction (%) rang (46.94 – 93.59), also the other samples Chitosan and Chitosan/Cinnamon that have reduction (%)

rang (11.87 – 62.50), so the sample Chitosan/Ginger and Chitosan/Curcumin acts as promising antimicrobial agent.

3.6. Mechanical properties

Fig. 10 depicts the characteristic stress–strain mechanical response (tensile strength–strain) of pure Chitosan and Chitosan doped by Ginger, Curcumin, and Cinnamon samples. The study indicated that all doped sample had higher tensile strength than pure chitosan. The addition of Ginger, Curcumin, and Cinnamon samples improved tensile strength, implying that the resulting samples interfacial properties have improved. Chitosan molecules have a lot of cyclic chain structures, which makes hydrogen bonding with –OH and –NH₂ groups easier to form. These bonds make rotation difficult, as well as other chain molecule movements, and are responsible for the chitosan film's mechanical properties. Ginger, Curcumin, and Cinnamon operate as chitosan molecules' interface coupling agents, forming higher-energy intermolecular interactions that encourage molecular chain rotation and boost the

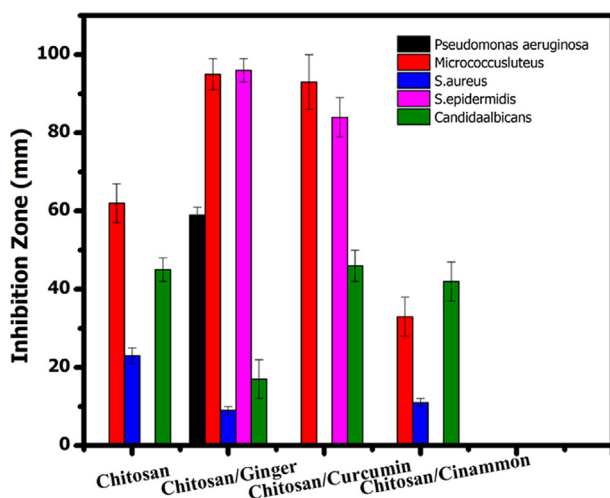


Fig. 9 Activity index of Chitosan, Chitosan/Ginger, Chitosan/Curcumin and Chitosan/Cinnamon against *Staphylococcus aureus*, *Staphylococcus epidermidis* and *Micrococcus luteus* via shake flask method.

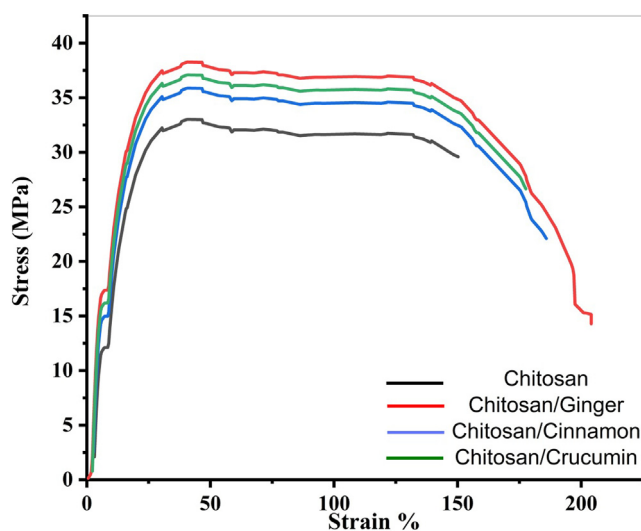


Fig. 10 Stress-strain curve of Chitosan, Chitosan/Ginger, Chitosan/Curcumin and Chitosan/Cinnamon.

tensile strength of the doped sample. The stress of pure Chitosan and Chitosan doped by Ginger, Curcumin, and Cinnamon samples are 32.8, 38.3, 36.9 and 35.8 MPa, respectively. It can be seen that Ginger has better tensile strength and elongation.

4. Conclusions

The structural characterization of chitosan blended with low cost and ecofriendly component as Ginger, Curcumin and Cinnamon is investigated using XRD, FTIR-ATR and FE-SEM to be used as antibacterial product. XRD, FTIR-ATR and FE-SEM curves confirmed the homogeneity between chitosan and other natural products and change in structural of chitosan. Optical properties of polymer blends are analyzed by

determining the optical parameters as Urbach tail and direct and indirect band gap and the results confirmed that the decrease of band gap and increasing Urbach tail by blended Chitosan with Ginger, Curcumin and Cinnamon which affirmed the creation of localized state and change in the band structure after blending. In addition, the antimicrobial activity of the prepared film were investigated using two methods (inhibition zone and shake flask methods) against Gram-positive microorganism [*Micrococcus luteus*, *Staphylococcus aureus*, and *Staphylococcus epidermidis*], Gram-negative microorganism [*Pseudomonas aeruginosa*], and pathogenic yeast [*Candida albicans*]. Chitosan/ Ginger has better tensile strength and elongation. The shake flask method gives effects compared to inhibition zone method and showing that Chitosan/Ginger give high antimicrobial activity toward Gram-positive microorganism compared to pure chitosan that make it used for medical applications.

Data availability

The datasets generated during and/or analyzed during the current study are available from the corresponding author on reasonable request.

Ethical approval

This article does not contain any studies with human participants or animals performed by any of the authors.

Acknowledgements

The authors extend their appreciation to the Deanship of Scientific Research at King Khalid University for supporting this work through research groups program under grant number R.G.P.2/120/42. This work was supported by Taif University Researchers Supporting Project number (TURSP-2020/117), Taif University, Taif, Saudi Arabia.

References

- Abdelghaffar, F., Abdelghaffar, R.A., Arafa, A.A., Kamel, M.M., 2018. Functional antibacterial finishing of woolen fabrics using ultrasound technology. *Fibers and Polymers* 19 (10), 2103–2111.
- Ah, R., Fm, S., Sm, A., 2014. Active ingredients of ginger as potential candidates in the prevention and treatment of diseases via modulation of biological activities. *International Journal of Physiology, Pathophysiology and Pharmacology* 6 (2), 125–136.
- Allan, C.R., Hadwiger, L.A., 1979. The fungicidal effect of chitosan on fungi of varying cell wall composition. *Experimental mycology* 3 (3), 285–287.
- Amalraj, A., Raj, K.J., Haponiuk, J.T., Thomas, S., Gopi, S., 2020. Preparation, characterization, and antimicrobial activity of chitosan/gum arabic/polyethylene glycol composite films incorporated with black pepper essential oil and ginger essential oil as potential packaging and wound dressing materials. *Advanced Composites and Hybrid Materials* 3 (4), 485–497.
- Aziz, S., 2017. Morphological and Optical Characteristics of Chitosan (1-x): Cu₀x (4 ≤ x ≤ 12) Based Polymer Nano-Composites: Optical Dielectric Loss as an Alternative Method for Tauc's Model. *Nanomaterials* 7 (12), 444.
- Bonilla, J., Sobral, P., 2017. Antioxidant and antimicrobial properties of ethanolic extracts of guarana, boldo, rosemary and cinnamon. *Brazilian Journal of Food Technology* 20.

- Chakraborty, S., & Ilagan, A. P. D. 2020. Chitosan Curcumin Film As A Sensor For Detection of O-Nitrophenol and Fluoride Ion Using Fluorescence Quenching Technique.
- Chen, X., Zou, L., Niu, J., Liu, W., Peng, S., Liu, C., 2015. The Stability, Sustained Release and Cellular Antioxidant Activity of Curcumin Nanoliposomes. *Molecules* 20 (8), 14293–14311. <https://doi.org/10.3390/molecules200814293>.
- Choo, K., Ching, Y.C., Chuah, C.H., Julai, S., Liou, N.S., 2016. Preparation and characterization of polyvinyl alcohol-chitosan composite films reinforced with cellulose nanofiber. *Materials* 9 (8), 644.
- Dhivya, S., Padma, V.V., Santhini, E., 2015. Wound dressings—a review. *BioMedicine* 5 (4), 1–5.
- Duan, Z., Li, C., Ding, W., Zhang, Y., Yang, M., Gao, T., Cao, H., Xu, X., Wang, D., Mao, C., 2021. Milling force model for aviation aluminum alloy: academic insight and perspective analysis. *Chinese Journal of Mechanical Engineering* 34, 1–35.
- Feng, Y., Li, F., Yan, J., Guo, X., Wang, F., Shi, H., Du, J., Zhang, H., Gao, Y., Li, D., Yao, Y., Hu, W., Han, J., Zhang, M., Ding, R., Wang, X., Huang, C., Zhang, J., 2021. Pan-cancer analysis and experiments with cell lines reveal that the slightly elevated expression of DLGAP5 is involved in clear cell renal cell carcinoma progression. *Life Sciences* 287, 120056.
- Gao, T., Li, C., Zhang, Y., Yang, M., Jia, D., Jin, T., Hou, Y., Li, R., 2019. Dispersing mechanism and tribological performance of vegetable oil-based CNT nanofluids with different surfactants. *Tribology International* 131, 51–63.
- Guo, Y., Zhang, Y., Luo, D., Ma, T., 2013. Raw Ginger Composite Antioxidant with High Efficiency to Extract Vitamin C from Strawberry. *Advances In Chemical Engineering And Science* 03 (03), 185–188.
- Irawan, A., Barleany, D. R., Jayanudin, Yulvianti, M., Maulana, R. C., & Fitriani, L. Y. 2019, March. Chitosan active films containing red ginger extract for shelf-life extension and quality retention of milkfish (*chanos chanos*). In AIP Conference Proceedings (Vol. 2085, No. 1, p. 020032). AIP Publishing LLC.
- Ismail, E., Sabry, D., Mahdy, H., Khalil, M., 2014. Synthesis and Characterization of some Ternary Metal Complexes of Curcumin with 1,10-phenanthroline and their Anticancer Applications. *Journal Of Scientific Research* 6 (3), 509–519.
- Ji, X., Hou, C., Shi, M., Yan, Y., Liu, Y., 2020. An Insight into the Research Concerning *Panax ginseng* C. A. Meyer Polysaccharides: A Review. *Food reviews international*, 1–17.
- Ji, Xiaolong, Peng, Baixiang, Ding, Hehui, Cui, Bingbing, Nie, Hui, Yan, Yizhe, 2021. Purification, Structure and Biological Activity of Pumpkin Polysaccharides: A Review. *Food Reviews International*, 1–13.
- Kenawy, E.R., Worley, S.D., Broughton, R., 2007. The chemistry and applications of antimicrobial polymers: a state-of-the-art review. *Biomacromolecules* 8 (5), 1359–1384.
- Lin, X., Li, Z., Liang, B., Zhai, H., Cai, W., Nan, J., et al. 2019. Accelerated microbial reductive dechlorination of 2,4,6-trichlorophenol by weak electrical stimulation, 162, 236-245. doi: 10.1016/j.watres.2019.06.068.
- Li, H., Wang, F., 2021. Core-shell chitosan microsphere with antimicrobial and vascularized functions for promoting skin wound healing. *Materials & design* 204, 109683.
- Liu, M., Li, C., Cao, C., Wang, L., Li, X., Che, J., Yang, H., Zhang, X., Zhao, H., He, G., 2021. Walnut fruit processing equipment: academic insights and perspectives. *Food Engineering Reviews* 13, 822–857.
- Liu, D., Wei, Y., Yao, P., Jiang, L., 2006. Determination of the degree of acetylation of chitosan by UV spectrophotometry using dual standards. *Carbohydrate Research* 341 (6), 782–785.
- M, Y., & PR, I. 2019. Chitosan Based Films Incorporated with Turmeric/Clove/Ginger Essential Oil for Food Packaging. *Journal of Nanomedicine & Nanotechnology*, 10(5).
- Matica, M.A., Achmann, F.L., Tøndervik, A., Sletta, H., Ostafe, V., 2019. Chitosan as a wound dressing starting material: Antimicrobial properties and mode of action. *International journal of molecular sciences* 20 (23), 5889.
- McFarland, J., 1907. The nephelometer: an instrument for estimating the number of bacteria in suspensions used for calculating the opsonic index and for vaccines. *Journal of the American Medical Association* 49 (14), 1176–1178.
- Menazea, A., Ismail, A., Awwad, N., Ibrahim, H., 2020. Physical characterization and antibacterial activity of PVA/Chitosan matrix doped by selenium nanoparticles prepared via one-pot laser ablation route. *Journal of Materials Research And Technology* 9 (5), 9598–9606.
- Mohseni-Bandpi, A., Kakavandi, B., Kalantary, R.R., Azari, A., Keramati, A., 2015. Development of a novel magnetite–chitosan composite for the removal of fluoride from drinking water: adsorption modeling and optimization. *Rsc Advances* 5 (89), 73279–73289.
- Mostafa, F.A., Abd El Aty, A.A., Hamed, E.R., Eid, B.M., Ibrahim, N.A., 2016. Enzymatic, kinetic and anti-microbial studies on *Aspergillus terreus* culture filtrate and *Allium cepa* seeds extract and their potent applications. *Biocatalysis and Agricultural Biotechnology* 5, 116–122.
- Mott, N.F., Davis, N.F., 1979. *Electronic process in non-crystalline materials*. Oxford University Press, USA.
- Motterlini, R., Foresti, R., Bassi, R., Green, C., 2000. Curcumin, an antioxidant and anti-inflammatory agent, induces heme oxygenase-1 and protects endothelial cells against oxidative stress. *Free Radical Biology And Medicine* 28 (8), 1303–1312. [https://doi.org/10.1016/s0891-5849\(00\)00294-x](https://doi.org/10.1016/s0891-5849(00)00294-x).
- Nabavi, S., Di Lorenzo, A., Izadi, M., Sobarzo-Sánchez, E., Daglia, M., Nabavi, S., 2015. Antibacterial Effects of Cinnamon: From Farm to Food. *Cosmetic and Pharmaceutical Industries. Nutrients* 7 (9), 7729–7748.
- Olafadehan, O., Abbulimen, K., Adeleke, A., Njoku, C., Amoo, K., 2019. Production and characterization of derived composite biosorbents from animal bone. *African Journal of Pure And Applied Chemistry* 13 (2), 12–26.
- Rachtanapun, P., Klunklin, W., Jantrawut, P., Jantanasakulwong, K., Phimsiripol, Y., Seesuriyachan, P., Leksawasdi, N., Chaiyasao, T., Ruksiriwanich, W., Phongthai, S., Sommano, S.R., Punyodom, W., Reungsang, A., Ngo, T.M.P., 2021. Characterization of chitosan film incorporated with curcumin extract. *Polymers* 13 (6), 963.
- Rehim, M.H.A., Yassin, M.A., Zahran, H., Kamel, S., Moharam, M. E., Turky, G., 2020. Rational design of active packaging films based on polyaniline-coated polymethyl methacrylate/nanocellulose composites. *Polymer Bulletin* 77 (5), 2485–2499.
- Salim, A., Bidin, N., 2017. Pulse Q-switched Nd:YAG laser ablation grown cinnamon nanomorphologies: Influence of different liquid medium. *Journal Of Molecular Structure* 1149, 694–700.
- Singh, P., Wani, K., Kaul-Ghanekar, R., Prabhune, A., Ogale, S., 2014. From micron to nano-curcumin by sophorolipid co-processing: highly enhanced bioavailability, fluorescence, and anti-cancer efficacy. *RSC Adv.* 4 (104), 60334–60341.
- Subhan, M., Alam, K., Rahaman, M., Rahman, M., Awal, R., 2014. Synthesis and Characterization of Metal Complexes Containing Curcumin (C₂₁H₂₀O₆) and Study of their Anti-microbial Activities and DNA Binding Properties. *Journal of Scientific Research* 6 (1), 97–109.
- Valand, N., Patel, M., Menon, S., 2015. Curcumin-p-sulfonatocalix resorcinarene (p-SCR) interaction: thermo-physico chemistry, stability and biological evaluation. *RSC Advances* 5 (12), 8739–8752.
- Wang, Y., Li, C., Zhang, Y., Yang, M., Li, B., Dong, L., Wang, J., et al, 2018. Processing characteristics of vegetable oil-based nanofluid MQL for grinding different workpiece materials. *International Journal of Precision Engineering and Manufacturing-Green Technology* 5, 327–339.

- Wang, Z., Xiang, H., Dong, P., Zhang, T., Lu, C., Jin, T., Chai, K.Y., 2021. Pegylated azelaic acid: Synthesis, tyrosinase inhibitory activity, antibacterial activity and cytotoxic studies. *Journal of Molecular Structure* 1224, 129234.
- Yan, Y., Feng, L., Shi, M., Cui, C., Liu, Y., 2020. Effect of plasma-activated water on the structure and in vitro digestibility of waxy and normal maize starches during heat-moisture treatment. *Food chemistry* 306, 125589.
- Yang, Mengmeng, Kong, Qingquan, Feng, Wei, Yao, Weitang, Wang, Qingyuan, 2021. Hierarchical porous nitrogen, oxygen, and phosphorus ternary doped hollow biomass carbon spheres for high-speed and long-life potassium storage. *Carbon energy*. <https://doi.org/10.1002/cey2.157>.
- Yang, M., Li, C., Zhang, Y., Jia, D., Zhang, X., Hou, Y., Li, R., Wang, J., 2017. Maximum undeformed equivalent chip thickness for ductile-brittle transition of zirconia ceramics under different lubrication conditions. *International Journal of Machine Tools and Manufacture* 122, 55–65.
- Yaseen, S., Taqa, A., Al-Khatib, A., 2020. The effect of incorporation Nano Cinnamon powder on the shear bond of the orthodontic composite (an in vitro study). *Journal of Oral Biology And Craniofacial Research* 10 (2), 128–134.
- Yashaswini, M., Iyer, P., 2019. Chitosan Based Films Incorporated with Turmeric/Clove/Ginger Essential Oil for Food Packaging. *J Nanomed Nanotech* 10, 537.
- Zhang, Y., Li, C., Jia, D., Li, B., Wang, Y., Yang, M., Hou, Y., Zhang, X., 2016. Experimental study on the effect of nanoparticle concentration on the lubricating property of nanofluids for MQL grinding of Ni-based alloy. *Journal of Materials Processing Technology* 232, 100–115.
- Zhang, L., Wang, L., Zhang, Y., Wang, D., Guo, J., Zhang, M., Li, Y., 2022. The performance of electrode ultrafiltration membrane bioreactor in treating cosmetics wastewater and its anti-fouling properties. *Environmental Research* 206, 112629.
- Zhang, C., Zhang, C., Liu, C., Luo, X., 2021. Characterization of the Complete Mitochondrial Genome of *Acanthacorydalid fruhstorferi* van der Weele (Megaloptera: Corydalidae). *Journal of the Kansas Entomological Society* 93 (4), 306–314.
- Zou, Q., Xing, P., Wei, L., Liu, B., 2019. Gene2vec: gene subsequence embedding for prediction of mammalian N⁶-methyladenosine sites from mRNA. *RNA (Cambridge)* 25 (2), 205–218. <https://doi.org/10.1261/rna.069112.118>.